Supporting Information

Nanocomposite Architecture for Rapid, Spectrally-Selective Electrochromic Modulation of Solar Transmittance

Jongwook Kim,[†] *Gary K. Ong,*[†,‡] *Yang Wang,*[†] *Gabriel LeBlanc,*[†] *Teresa E. Williams,*[§,∥] *Tracy M. Mattox,*[∥] *Brett A. Helms,*[∥] *Delia J. Milliron**[,†]

† McKetta Department of Chemical Engineering, University of Texas at Austin, Austin, Texas 78712, United States

‡ Department of Materials Science & Engineering, University of California, Berkeley, Berkeley, California 94720, United States

§ Graduate Group in Applied Science & Technology, University of California, Berkeley, Berkeley, California 94720, United States

∥ The Molecular Foundry, Lawrence Berkeley National Laboratory, Berkeley, California 94720, United States

*email: milliron@che.utexas.edu

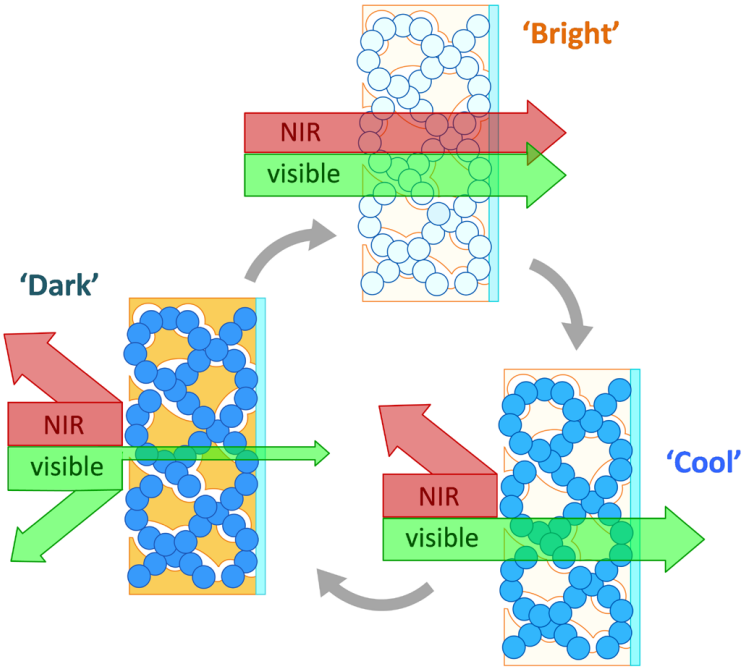

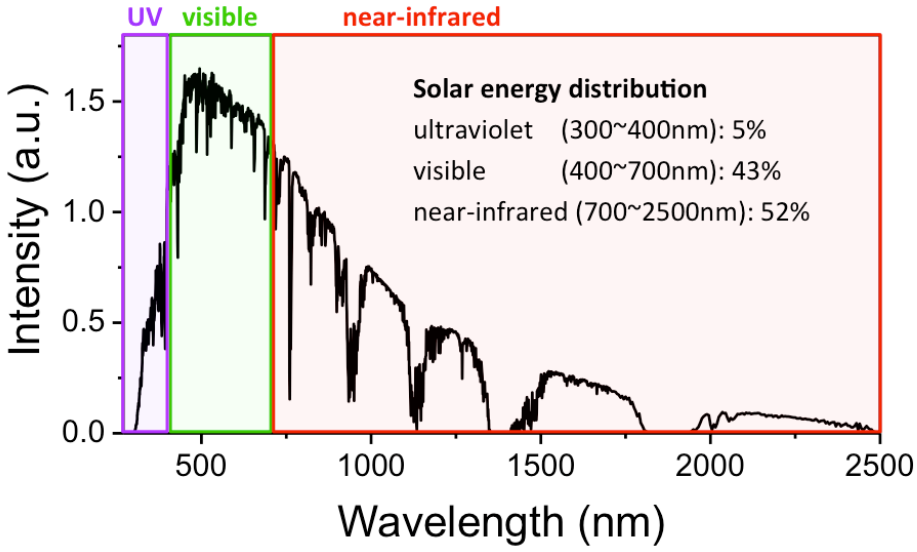

Figure S1. Normalized solar radiation intensity spectrum.
Ultraviolet (UV), visible (VIS), and near-infrared (NIR) regions are indicated respectively as purple, green, and red color. The localized surface plasmon resonance (LSPR) spectrum of WO_{3-x} nanocrystal (Figure 1c in the main text) overlaps well with the NIR region of this spectrum.

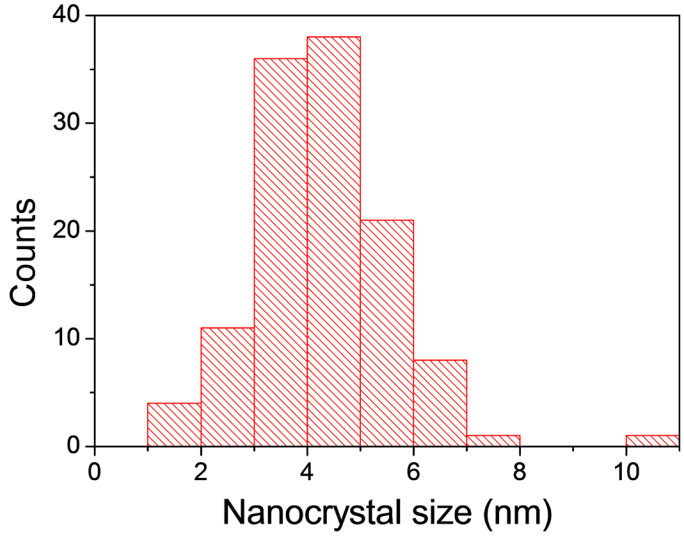

Figure S2. WO_{3-x} nanocrystal size distribution.
Histogram of the WO_{3-x} nanocrystal size manually measured from the TEM images (Figure 1a in the main text). The average size obtained from 120 counts is 4.3 +/- 1.3 nm.

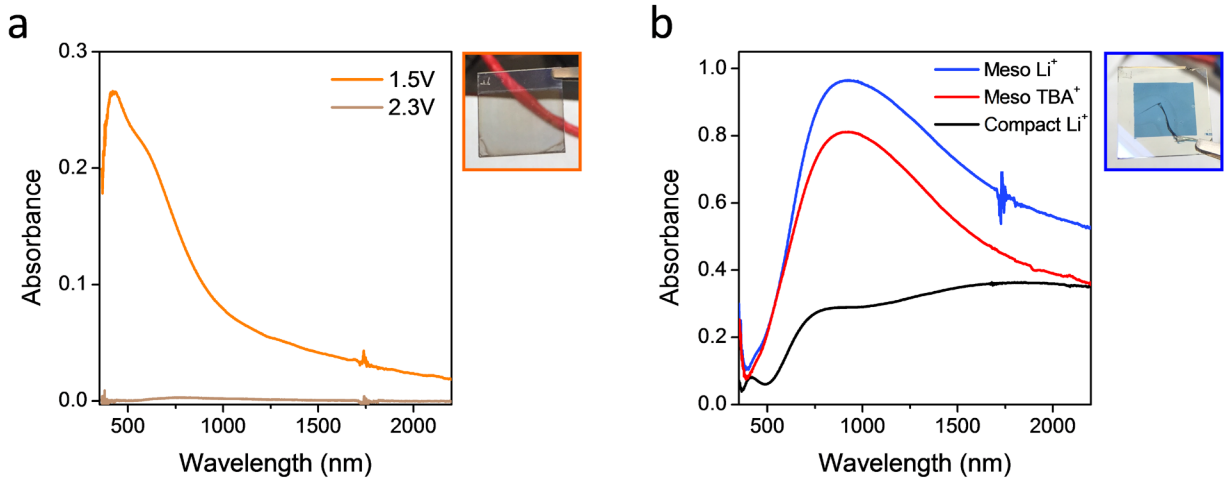

Figure S3. Electrochemically switched optical spectra of electrochromic films.

a) Absorbance spectra of a pure NbO_x glass film collected after saturation at 1.5 V (orange) and 2.3 V (brown) versus Li reference electrode in Li-TFSI electrolyte. The measurement was baselined with the same sample at the fully bleached state at 4 V. The film was prepared with the same condition used for the NbO_x in-filling of the composite film demonstrated in Figure 3a in the main text. It is clearly shown that NbO_x does not optically switch at 2.3 V, which allows dual-band modulation in the composite film. The right picture was taken after fully charging at 1.5 V and shows a moderate darkening of NbO_x in the visible (VIS) range.

b) Absorbance spectra of pure WO_{3-x} nanocrystal films. Blue line is for a mesoporous film prepared by the block copolymer templated assembly (thickness=280 nm, porosity=71%), switched in Li-TFSI electrolyte. Red line is for the same sample switched in TBA-TFSI electrolyte thus in the purely capacitive regime. Black line is for a randomly packed film (saturated at 1.5 V) prepared with the same volume of WO_{3-x} nanocrystals per unit area (thickness=108 nm, porosity=28%). The right picture was taken after full charging (1.5 V *vs.* Li/Li^+) of a mesoporous film sample.

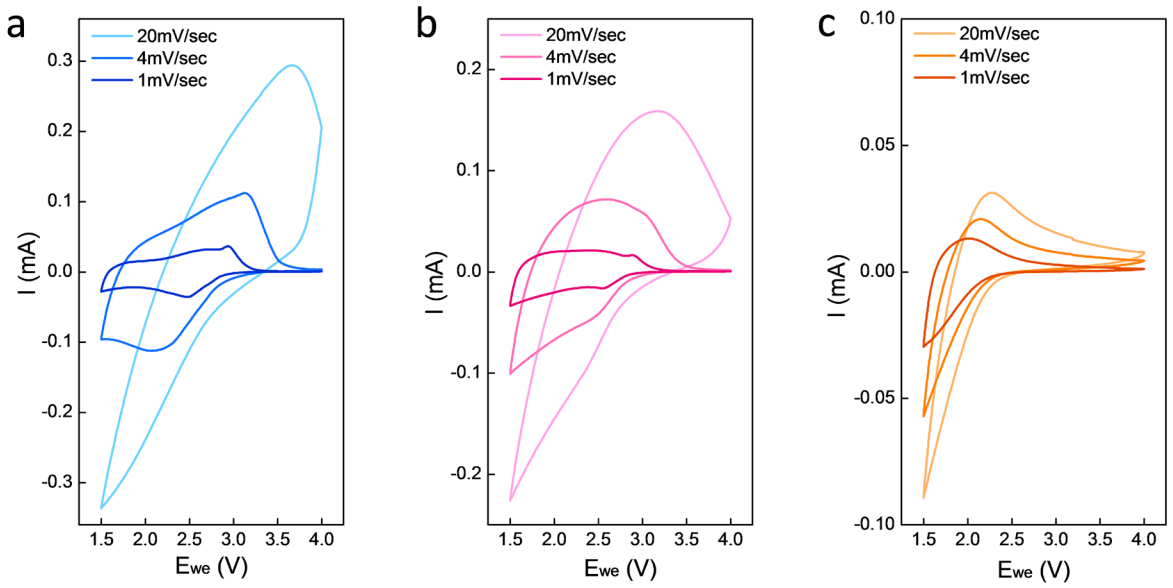

Figure S4. Cyclic voltammetry.

Cyclic voltammetry (CV) plots with three different sweep rates (1, 4, and 20 mV/sec) for a) mesoporous assembled pure WO_{3-x} film, b) architected WO_{3-x}-NbO_x composite film, and c) pure NbO_x glass film. The large capacitive contribution in pure WO_{3-x} film is shown in the fast sweep rate (20mV/sec) plot in (a). In the plots for 1mV/sec, where the capacitive contribution is minimized, it is clearly shown that WO_{3-x} has a reduction (Li^+ intercalation) peak near 2.5V where NbO_x is still inactive. The significant charging currents for WO_{3-x} above this voltage both in capacitive and reductive routes allow the dual-band modulation by independent switching of WO_{3-x} and NbO_x at different voltages. The film thickness and the active surface area were 420nm and 1.64cm^2, 173nm and 0.63cm^2, and 120nm and 0.63cm^2 respectively for (a), (b), and (c).

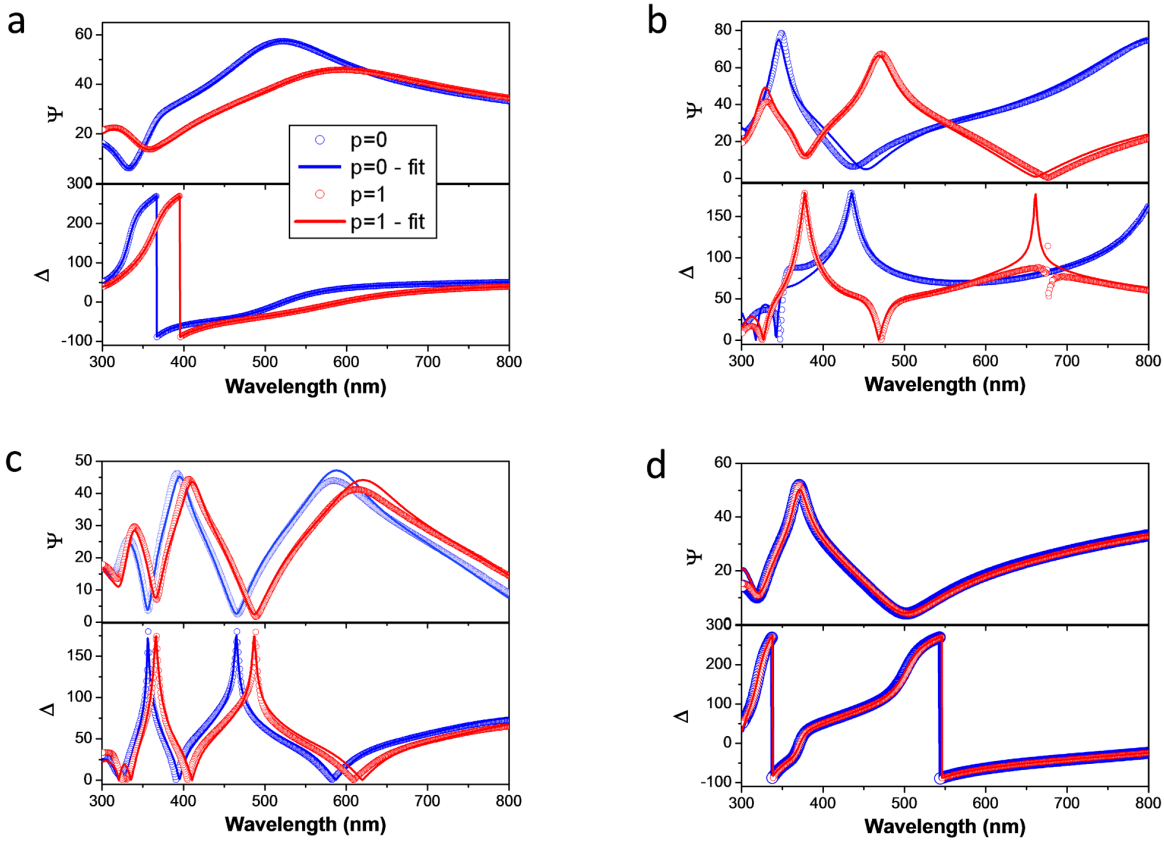

Figure S5. Ellipsometric porosimetry data and fitting.

Ψ and Δ spectra obtained at the two extreme toluene isotherms with the relative vapor pressure (p) being 0 (blue circles) and 1 (red circles), and their theoretically fitted lines by using Lorentz oscillator model and Cauchy dispersion law for a) randomly packed WO_{3-x} nanocrystal film, b) assembled mesoporous pure WO_{3-x} nanocrystal film (Figure 2a-c in the main text), c) architected WO_{3-x}-NbO_x composite film (Figure 2d-f in the main text), and d) pure NbO_x glass film.

A moderate spectral shift in a) indicates the typical moderate porosity of randomly packed nanocrystal films (measured porosity = 28%, Table 1 in the main text) and the large shift in b) corresponds to the large porosity of 71% due to the block copolymer templated mesoporous assembly. The zero-shift in d) indicates that NbO_x glass film is compact without pores, and the little shift in c) together with the pore radius distribution (Figure 2d-f in the main text) implies the efficient NbO_x in-filling and generation of the small pore channels.

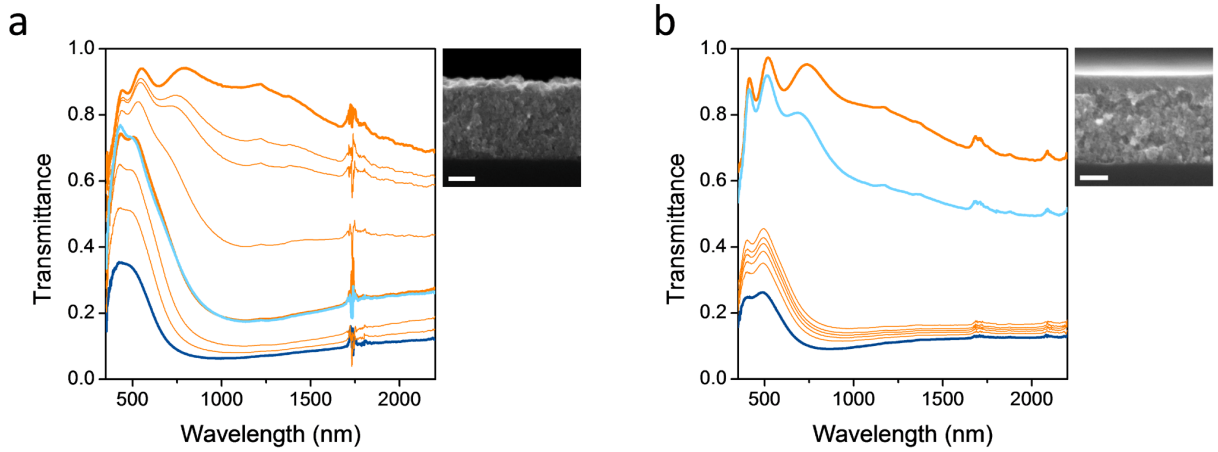

Figure S6. Optical switching kinetics of WO_{3-x}-NbO_x composite films.

a) Transmittance spectral evolution of the architected WO_{3-x}-NbO_x composite film of which the WO_{3-x} framework and the mesopore channels are exposed to the film surface (cross section SEM of the film at the right). Light blue line is a "cool mode" spectrum acquired 3 minutes after applying 2.3 V from a "bright mode" (thick orange line). And the dark blue line is a 'dark mode' spectrum obtained after 10 minutes of applying 1.5 V. The thin orange lines were collected at each 30 seconds after applying 4 V from the 'dark mode'. A fast bleaching in the VIS range, thus fast discharging of NbO_x, turned the film back to the 'cool mode' within 90 seconds and a followed fast discharging of WO_{3-x} allowed a full bleaching to the 'bright mode' in another two minutes, which is consistent with the fast discharging kinetics shown in Figure 3b in the main text.

b) Transmittance spectra acquired from the same switching experiment as a) on a composite film with the same architecture but with a 40nm-thick NbO_x overlayer which closes the pore channels (cross section SEM of the film at the right). In this case, 'cool mode' performance is poor (the light blue line is a saturated spectrum at 2.3 V) because WO_{3-x} – now covered with NbO_x – could not be switched independently. When applying 1.5 V, the transmittance in VIS and NIR ranges decreased simultaneously as both WO_{3-x} and NbO_x were charged together. The thin orange lines here were collected at 30, 60, 90, 120, and 180 seconds after applying 4 V from the 'dark mode', and it took about 10 hours to fully bleach this sample back to the 'bright mode' constantly applying 4 V.

Methods

WO_{3-x} nanocrystal synthesis – 20 mL of oleic acid (Aldrich) was mixed with 2 mL of oleylamine (Aldrich) and degased under vacuum at 120°C for one hour. 340 mg of tungsten(IV) chloride (WCl_4) powder was stirred in 4 mL of oleic acid and injected into the solvent mixture heated to 300°C. The reaction quickly turned to dark blue color and was cooled to room temperature 10 minutes after the injection. The solution was transferred into a glove box, precipitated by adding an excess volume of isopropyl alcohol (Aldrich), centrifuged, and the collected pellet was dispersed in 10 mL of hexane (Aldrich). Then, the organic surface coordinating ligands were stripped by using Meerwein's reagent – triethyloxonium tetrafluoroborate (Aldrich) based on the method reported previously[1]. Briefly, 50 mg of Meerwein's reagent was dissolved in 5 mL of acetonitrile (Aldrich), mixed with 1 mL of WO_{3-x} solution in hexane (10 mg/mL), stirred overnight, and then the precipitated stripped nanocrystals were re-dispersed in DMF (Aldrich).

$PDMA_{10k}$-*b*-PS_{60k} block copolymer (BCP) and **decaniobate-POMs ($[Nb_{10}O_{28}]^{6-}$)** were synthesized according to the methods reported by us previously[2, 3].

Block copolymer templated assembly of WO_{3-x} – The WO_{3-x} nanocrystal framework was assembled based on the original method established by us previously[2, 4]. Briefly, the block copolymer micelle solution was prepared by slowly mixing 200μL of ethanol with 100μL of $PDMA_{10k}$-*b*-PS_{60k} solution (60 mg/mL) in DMF. Then 100μL of the stripped WO_{3-x} nanocrystal solution (70 mg/mL) in DMF was added. This solution was spin-coated (800 rpm) three times on ITO-coated glass substrates (Diamond Coatings Limited, 20 mm × 20 mm × 1.1 mm, 200 Ω/sq sheet resistance) and then annealed in air at 400°C for one hour to remove micelles.

NbO_x glass in-filling – An aqueous ethanol (1:1 mixture) solution of the Nb-POM was spin-coated (2000 rpm) on the prepared WO_{3-x} nanocrystal framework film. The POM concentration was delicately adjusted to fill the whole mesopore volume but not to leave an overlayer on the top surface of the nanocrystal film (ex. 140 mg/mL for a 260 nm thick composite film). The composite film was then annealed in air at 400°C for 30 minutes to decompose POMs and condense into NbO_x glass generating the interfacial pore channels.

Unstructured pure WO_{3-x} nanocrystal films were deposited by spin-coating the stripped nanocrystal solution in DMF followed by the same annealing procedure as for the architected films (400°C-1hour in air).

Pure NbO_x glass films were prepared in the same way described above for in-filling on bare substrates without WO_{3-x} framework.

Transmission electron microscopy (TEM) – The TEM image of the WO_{3-x} colloidal solution was acquired on a JEOL-2010F with a sample prepared by drying a drop of diluted hexane

solution on the surface of a holey carbon-coated copper grid. The nanocrystal size was taken from the statistics on 120 particles on the TEM image.

X-ray diffraction (XRD) – The XRD pattern of the WO_{3-x} nanocrystals was acquired on a Rigaku R-axis Rapid II diffractometer with copper K-alpha radiation. The XRD sample was prepared by drying several drops of concentrated toluene solution on a silicon wafer substrate.

Scanning electron microscopy (SEM) – SEM imaging of the film samples were carried out on Zeiss Gemini Supra-40 microscope with the samples prepared on silicon wafer substrates. The film thicknesses were determined by cross-section imaging.

Ellipsometric porosimetry (EP) – EP data were acquired on a SEMILAB PS-1100R ellipsometric porosimeter and analyzed with the accompanied SEA software (spectroscopic ellipsometry data analysis). Electochromic film samples for EP were prepared by spin-coating as described above on un-doped Si-wafer substrates.

UV-Vis-NIR spectroscopy – The absorbance spectra of WO_{3-x} nanocrystals were collected on an Agilent-Cary5000 spectrophotometer with a sample prepared by diluting the toluene solution of nanocrystals in tetrachloroethylene (~0.2 mg/mL, beam path length = 1 cm). The transmittance and absorbance spectra of the film samples were collected on an ASD Quality Spec Pro visible–NIR spectrometer.

Electrochromic modulation – A homebuilt spectroelectrochemical cell installed in a glove box was used for the electrochemical operations and the in-situ optical measurements. The WO_{3-x}, NbO_x, and WO_{3-x}-NbO_x composite films were placed as working electrodes in the cell connected to the spectrometer and the light source with fiber-optic cables. For the standard Li^+ ion charging experiment, three-electrode configuration with a single Li foil as counter and reference electrodes was used with 0.1 M Li-TFSI (Aldrich) in tetraglyme (Aldrich) as electrolyte. For the purely capacitive charging experiment, a Pt foil counter electrode and a Ag/Ag^+ reference electrode, calibrated against a Li foil reference electrode (+3.0 V), were used with 0.1M TBA-TFSI (Aldrich) in propylene carbonate to prevent Li^+ ion contamination (Aldrich). A Bio-logic VMP3 potentiostat was used for chronoamperometry (CA) and cyclic voltammetry (CV) studies, and the optical transmission spectra were collected in-situ. The cycling stability was measured upon CV cycling in between 1.5~4 V (vs. Li) with the sweep rates selected to obtain the charge capacity above 70% of the saturated values under CA in between 1.5~4 V (30 mV/sec for pure WO_{3-x}, 20 mV/sec for WO_{3-x}-NbO_x composite, and 10 mV/sec for pure NbO_x). The charge capacities measured during charging and discharging were identical for each cycle.

[1] Rosen, E. L.; Buonsanti, R.; Llordes, A.; Sawvel, A. M.; Milliron, D. J.; Helms, B. A. *Angew. Chem. Int. Ed.* **51**, 684-689, (2012).

[2] Buonsanti, R.; Pick, T. E.; Krins, N.; Richardson, T. J.; Helms, B. A.; Milliron, D. J. *Nano Lett.* **12**, 3872-3877, (2012).

[3] Llordes, A.; Hammack, A. T.; Buonsanti, R.; Tangirala, R.; Aloni, S.; Helms, B. A.; Milliron, D. J. *J. Mater. Chem.* **21**, 11631-11638, (2011).

[4] Williams, T. E.; Chang, C. M.; Rosen, E. L.; Garcia, G.; Runnerstrom, E. L.; Williams, B. L.; Koo, B.; Buonsanti, R.; Milliron, D. J.; Helms, B. A. *J. Mater. Chem. C* **2**, 3328-3335, (2014).